INTEGRATED PROCESSING OF TERRESTRIAL LASER SCANNER DATA AND FISHEYE-CAMERA IMAGE DATA

D. Schneider, E. Schwalbe

Technische Universität Dresden, Institute of Photogrammetry and Remote Sensing, 01062 Dresden, Germany - (danilo.schneider, ellen.schwalbe)@tu-dresden.de

TS-68: SS-16 – Terrestrial Laser Scanning Calibration Techniques

KEY WORDS: Laser scanning, fisheye lens, bundle adjustment, calibration, registration

ABSTRACT:

The paper presents the integration of a geometric model of fisheye lenses and a geometric terrestrial laser scanner model in a bundle block adjustment. The model allows for a full integration of hemi-spherical fisheye imagery into terrestrial laserscanner data processing schemes. Both the laserscanner and fisheye geometric model are extended by additional parameters to compensate for deviations from the ideal model and to optimize the accuracy potential. The results of the combined bundle adjustment are analyzed and the advantages of the proposed approach will be discussed in detail. For this purpose, several laser scans with a Riegl LMS-Z420i as well as several fisheye images were recorded in a calibration room equipped with ca. 100 reference points. The laser scans and the fisheye images were processed in different configurations, the resulting standard deviation of the calculated object point coordinates are analyzed and compared. Finally the calibration results of both terrestrial laser scanner and fisheye lens camera as well as the accuracy of the observations resulting from the variance component estimation will be presented. The results show that the 3D coordinate determination precision can be enhanced significantly by the integrated processing, and that scanner and camera aid one another in the self-calibration.

1. INTRODUCTION

The combination of terrestrial laser scanner and image data presents an interesting option in many applications, as both types of data can be used for the analysis simultaneously and their properties are largely complementary (e.g. Jansa et. al., 2004; Rönnholm et. al., 2007). While a laser scanner produces precise and reliable 3D information, cameras record colour information with a high visual interpretability and a high lateral resolution and accuracy. The combination of point clouds and image information is therefore supported by several software packages. Besides the pure colorizing of point clouds, images are used to texturize 3D models for example in cultural heritage applications, or to facilitate the interpretation of complex point clouds in industrial applications. In each case a strict geometric description and subsequently a precise calibration are necessary for an accurate geometric referencing between laser scanner and image data.

Figure 1. Laser scanner and camera: Riegl LMS-Z420i with Nikon D100 (Riegl, 2007): FARO LS 880 with Nikon D200 and Fisheye lens (Faro, 2005); Nikkor Fisheye lens 8 mm

Terrestrial laser scanners, which are currently available on the market, are often classified by their field of view. There are camera-view scanners and panoramic-view scanners covering a 360° horizontal field of view. Many panoramic-view scanners allow for recording of nearly 180° vertically, which means the coverage of a full sphere (apart from the bottom area). If a digital camera is mounted on a laser scanner with a hemispheric field of view (Figure 1) in order to record image information simultaneously, only a fisheye lens camera is able to record the same vertical field of view in one image. Therefore the combination of a laser scanner and a hemi-spherical fisheye lens camera is desired (e.g. terrestrial laser scanner FARO LS 880 (Faro, 2005)). Early photogrammetric applications of fisheye lenses are presented in (Beers, 1997). The combination of laser scan data and image data in a bundle adjustment is a promising method concerning the accuracy of data registration, instrument (self-)calibration, reliability and precision of 3D object geometry determination. The integration of central perspective image and laser scanner data in a combined adjustment is also investigated in (Wendt & Heipke, 2006; Ullrich et. al., 2003). (Schneider & Maas, 2007) describe the integrated bundle adjustment of laser scanner data and 360° panoramic imagery.

2. GEOMETRIC MODELS

The combined processing of different scans and fisheye images requires a superior coordinate system, in which object points as well as the exterior orientation are defined. The transformation between this coordinate system and the individual coordinate system of each scan or image is given by:

$$\mathbf{X} = \mathbf{X_0} + \mathbf{R} \cdot \mathbf{x} \tag{1}$$

where **R** = Rotation matrix
x = Coordinate vector of an object point defined in the scanner or camera coordinate system (*x,y,z*)
X = Coordinate vector of an object point defined in the superior coordinate system (*X,Y,Z*)
$\mathbf{X_0}$ = Translation vector between scanner or camera coordinate system and superior coordinate system

2.1 Terrestrial laser scanner

The geometric model of terrestrial laser scanners used for the following investigations was already presented in [Schneider, 2007]. It bases on spherical coordinates (distance, horizontal and vertical angle) as observations (Figure 2, Equation 2).

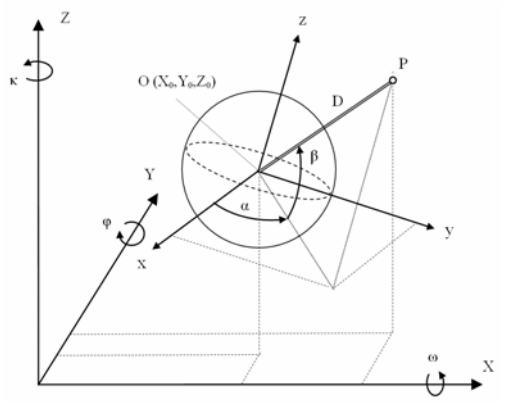

Figure 2. Geometric model of terrestrial laser scanners [Schneider, 2007]

$$\begin{aligned} D &= \sqrt{x^2 + y^2 + z^2} \\ \alpha &= \arctan\left(\frac{y}{x}\right) \\ \beta &= \arctan\left(\frac{z}{\sqrt{x^2 + y^2}}\right) \end{aligned} \tag{2}$$

Equation 2 can be extended by correction terms ΔD, $\Delta\alpha$, $\Delta\beta$ in order to compensate for systematic deviations from the basic model, which allows for the calibration of the laser scanner. The following additional parameters according to (Lichti, 2007) were included into the investigations presented in this paper:

- distance offset a_0 and scale a_1
- collimation and trunnion axis error b_1 and b_2
- vertical circle index error c_0
- horizontal and vertical circle eccentricity b_3, b_4 and c_1, c_2

The appropriate correction model is defined as follows (Lichti, 2007):

$$\begin{aligned} \Delta D &= a_0 + a_1 D \\ \Delta\alpha &= b_1 \sec\beta + b_2 \tan\beta + \left[b_3 \sin\alpha + b_4 \cos\alpha\right] \\ \Delta\beta &= c_0 + \left[c_1 \sin\beta + c_2 \cos\beta\right] \end{aligned} \tag{3}$$

Cyclic distance errors were not considered as the used laser scanner is a time-of-flight scanner, where cyclic errors are supposed to be not existent.

In comparison to the model described in (Lichti, 2007) two extra additional parameters were used in the geometric model, which could be determined significantly (Equation 4):

- eccentricity between collimation axis and vertical axis b_5
- eccentricity between collimation axis and trunnion axis c_3

$$\begin{aligned} \Delta\alpha_e &= \arcsin\frac{b_5}{D} \approx \frac{b_5}{D} \\ \Delta\beta_e &= \arcsin\frac{c_3}{D} \approx \frac{c_3}{D} \end{aligned} \tag{4}$$

Investigations of terrestrial laser scanners have shown that it is almost impossible to determine calibration values, which are effective and stable for the whole range and field-of-view as well as under different measurement conditions (e.g. Böhler & Marbs, 2004). In fact, correction values depend on a multitude of influences which can not be assumed to be invariable (object properties, area of distance, brightness, etc.). These circumstances can be considered by the implementation of a self-calibration procedure into the actual data processing.

Moreover, observations are often already pre-corrected in the laser scanner instrument using correction models which are not published. This fact causes additional problems regarding the determination of significant and stable calibration parameters.

2.2 Fisheye camera model

The geometry of the projection of fisheye lenses does not comply with the central perspective geometry. At TU Dresden, Institute of Photogrammetry and Remote Sensing, a strict geometric model for fisheye lenses was therefore developed and successfully implemented, which allows for the calibration and precise orientation of a camera with fisheye lens (Schwalbe, 2005).

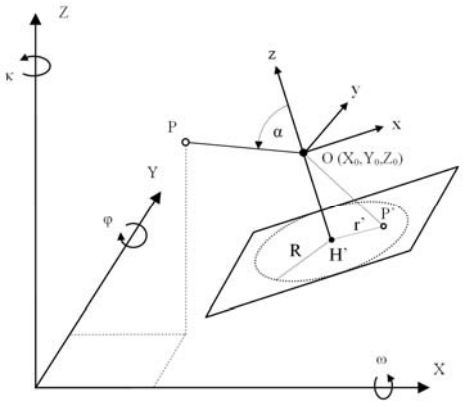

Figure 3. Geometric model of fisheye lens cameras

The model was extended by additional parameters for the compensation of remaining systematic errors, allowing the standard deviation of unit weight obtained from a spatial resection to be reduced to 0.1 pixels for a 14-Megapixel Kodak camera equipped with a Nikkor fisheye lens. Translated to object space, this corresponds to lateral accuracy of 1 mm at 10 m distance.

There are different fisheye projection geometries: Equi-distant, equi-solid-angle and orthographic projection (Ray, 1994; Backstein & Pajdla, 2002; Abraham & Förstner, 2005). The geometric concept is based on the dependence of the image radius *r'* and the angle of incidence α (Figure 3).

Experiments confirmed that the used fisheye lens complies best with the equi-solid-angle model. Therefore only this model will be described in the following. The image radius *r'* depends on the angle of incidence *α*:

$$r' = 2c \cdot \sin\frac{\alpha}{2} \quad \text{where} \quad \tan\alpha = \frac{\sqrt{x^2 + y^2}}{z} \tag{5}$$

In order to express the image observations *x'* and *y'* as function of the exterior and interior orientation as well as on the object point coordinates, equation (5) has to be introduced in the following equation, whose derivation is explained in detail in [Schwalbe & Schneider, 2005]:

$$\begin{aligned} x' &= x_0' + \frac{r'}{\sqrt{\left(\frac{y}{x}\right)^2 + 1}} + \Delta x' \\ y' &= y_0' + \frac{r'}{\sqrt{\left(\frac{x}{y}\right)^2 + 1}} + \Delta y' \end{aligned} \tag{6}$$

The correction terms Δ*x'* and Δ*y'* contain additional parameters for the compensation of radial-symmetric (A_1, A_2, A_3) and decentering (B_1, B_2) lens distortion (Brown, 1971) as well as affinity and shear of the image coordinate system (C_1, C_2) (El-Hakim, 1986):

$$\begin{aligned} \Delta x' &= x'(A_1 r'^2 + A_2 r'^4 + A_3 r'^6) + B_1(r'^2 + 2x'^2) + 2B_2 x' y' + C_1 x' + C_2 y' \\ \Delta y' &= y'(A_1 r'^2 + A_2 r'^4 + A_3 r'^6) + 2B_1 x' y' + B_2(r'^2 + 2y'^2) \end{aligned} \tag{7}$$

3. COMBINED BUNDLE BLOCK ADJUSTMENT

The geometric model of fisheye lens cameras was integrated into a bundle adjustment software package, which was originally developed and implemented for a combined analysis of laser scanner data and central-perspective or panoramic image data (Schneider & Maas, 2007).

The bundle adjustment software package supports the calculation as free network adjustment and handles outlier detection. Since different types of observations have to be adjusted simultaneously, it is necessary to assign adequate weights to the laser scanner and fisheye image observations. For this purpose a variance component estimation procedure was implemented in the adjustment. Thus, the precision characteristics of laser scanner and fisheye lens camera will be optimally utilised, and an improvement of the adjustment results can be achieved. Furthermore, this allows for a qualification of the measurements in terms of realistic accuracy values for fisheye lens data and laser scanner data.

4. PRACTICAL EXPERIMENTS

4.1 Calibration room

In order to practically assess the presented method, multiple laser scans and images with a fisheye lens camera were acquired in a test field, which is designed for the calibration of fisheye lenses (Schwalbe, 2005).

The test field is a room (4 × 5 × 3 m³), where 100 signalised object points are distributed at the surrounding walls and at the ceiling in a way that they form concentric circles on the fisheye image (Figure 4). Object point targets are designed as black circles (Ø 10 mm) on white background with a ring code, to allow for an automatic target detection and identification. The targets are orientated in a way that they face perpendicular to the centre of the room. Reference coordinates were determined using a common photogrammetric measurement system. However, the coordinates are only used as approximate values in the bundle adjustment and to define the superordinated coordinate system. The XY-plane of this coordinate system is orientated horizontal and the Z-axis is a vertical axis.

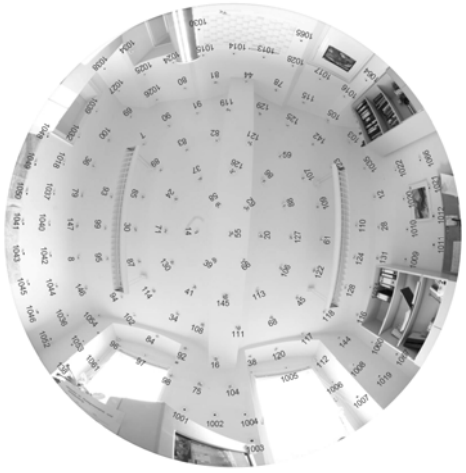

Figure 4. Fisheye image from the centre of the calibration room orthogonal to the ceiling with highlighted object point numbers

4.2 Laser scanner data

A terrestrial laser scanner Riegl LMS-Z420i was situated in each corner of the calibration room and tilted 45° vertically, in order to allow for the recording of points on the ceiling. Additionally, two scans from the centre of the room were recorded with a tilt angle of 90°. The laser scanner was also rotated 90° horizontally between both scans.

The angular resolution of the laser scans was 0.035°, which corresponds to a scan point distance of 2.5 mm in 4 m distance.

For the manual measurement of the target coordinates, the Riegl laser scanner software RiScan Pro was used. As the black circles on white background are well distinguishable within the intensity images of the laser scanner, these were used for the coordinate determination by manual selection of the target centre (with integer pixels) and attribution of the associated spherical coordinates. The target code can not be used because the quality of the laser scanner intensity images does not allow a code interpretation. Also an automatic target measurement with sub-pixel operators is not supported by the software. Therefore the lateral accuracy of the spherical laser scanner coordinates is strongly limited by the chosen angular resolution.

The target design (black on white background) turned out to be not really suitable, as the intensity values in the target centre were very low which often resulted in suboptimal accuracies of the distance determination. In some cases the laser scanner was not able to detect a reflected signal from the centre of the target. It has to be mentioned here, that white targets on black background would be better suitable for the laser scanner calibration. However, it has to be considered in principle, that the material and colour of the targets influences the distance measurement in a way, that distances will be measured systematically too short or too long. This fact has to be kept in mind for the interpretation of the calibration results, in particular regarding the parameters distance offset and scale.

4.3 Fisheye image data

In the calibration room mentioned above, five images with a 14-Megapixel Kodak DCS 14n Pro camera equipped with an 8 mm Nikkor fisheye lens were captured from different positions. With a pixel size of 8 µm the object resolution is 4 mm in 4 m distance.

Fisheye images are often characterized by strong effects of chromatic aberration ([Luhmann et. al., 2006], [van den Heuvel et. al., 2006]). Although the consideration of the chromatic aberration in the geometric model is basically possible (e.g. [Schwalbe, 2005]), this was not done in the investigations described in this paper. Instead, the images were divided into their three color channels, and only one channel (green) was used for the following analyses.

For the sub-pixel image point measurement within the hemispherical fisheye images and the decoding of point number the software Aicon 3D Studio was used.

4.4 Configurations and results

In the following, the results from different laser scanner and fisheye camera configurations, which have been processed in the integrated bundle block adjustment, will be analyzed. In order to achieve an optimal utilization of the different observation types, a variance component estimation scheme has been applied. Each calculation example is processed as free network adjustment and with an integrated self-calibration of the involved devices fisheye lens camera and terrestrial laser scanner.

4.4.1 Scans from the room centre

At first, two laser scans from the room centre (Figure 5, calculation a) and additionally one fisheye image (Figure 5, calculation b) were used to calculate the 3D coordinates of object point targets visible in each used scan or image. The combination of the two scans as well as the fisheye image provides almost the same field of view.

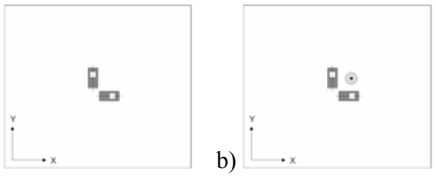

Figure 5. Configurations: scans from the room centre

For object points on the ceiling, X and Y coordinates can be considered as lateral coordinates, Z as the depth direction. Table 1 shows that the accuracy of the resulting object point coordinates (RMS of estimated standard deviations) can be improved using at least one fisheye image additionally, particularly in X and Y direction. This result was expected since the fisheye image observations were measured with sub-pixel accuracy operators (while the laser scanner observations result from integer pixel measurement within the intensity image). The standard deviation of object points resulting from the bundle adjustment of calculation b) is better than the used angular scan resolution and also better than the distance measurement accuracy.

	Scans/ Images	Observ./ Unknown	Points	RMS (mm) X	Y	Z	XYZ
a)	2 / 0	339 / 217	66	5.00	3.25	7.58	9.64
b)	2 / 1	457 / 233	66	2.69	2.00	4.47	5.59

Table 1. Bundle adjustment results (configuration a, b)

4.4.2 Two opposed scans

The purpose of the following calculations is to analyse, whether scans, which enclose optimal intersection angles with the object points, result in an improvement of the estimated accuracies. Therefore two diametrically opposed scans have been chosen (Figure 6, calculation c and d). Calculation e) and f) additionally utilize one fisheye image on each laser scanner position. In calculation g) and h), two scans and two fisheye images are distributed in the room corners to allow for optimal intersection geometry.

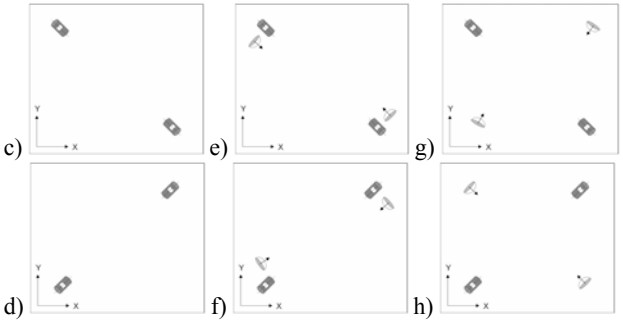

Figure 6. Configurations: diametrically opposed scans

Table 2 summarizes the results of the calculations illustrated in Figure 6. It has to be noted, that c) and d) are based on a lower number of corresponding object points visible in both scans due to object occlusions. However, the RMS values of these

calculations are clearly below those of calculation a) and b). This fact confirms that convergent laser scanner positions processed in a bundle adjustment help to increase the accuracy of object points. Moreover, the consideration of one fisheye image on each laser scanner position (calculation e and f) results in higher accuracies. The result of calculation g) and h) is slightly better, due to an even better overall intersection geometry.

	Scans/ Images	Observ./ Unknown	Points	RMS (mm) X	Y	Z	XYZ
c)	2 / 0	318 / 178	53	1.20	1.16	1.43	2.20
d)	2 / 0	306 / 172	51	0.97	1.00	1.22	1.85
e)	2 / 2	605 / 239	66	0.66	0.55	0.88	1.23
f)	2 / 2	585 / 239	66	0.61	0.60	0.67	1.09
g)	2 / 2	580 / 239	66	0.62	0.57	0.79	1.15
h)	2 / 2	582 / 239	66	0.54	0.49	0.68	1.00

Table 2. Bundle adjustment results (configuration c – h)

The results allow for the statement, that it is reasonable to use additional images in a combined bundle adjustment, in order to achieve a higher accuracy in terms of registration and instrument calibration. This applies particularly to fisheye images since they often cover the same field of view as the laser scanner. If the camera is actually mounted on the laser scanner, it is simple to use their images in a combined bundle adjustment, since an approximate orientation with respect to the laser scanner is already known.

4.4.3 Multiple scans from the room corners

In order to demonstrate the potential of the combined processing, observations of further scans and fisheye images were additionally introduced into the bundle adjustment (Figure 7). For this purpose, at first i) 4 and j) 6 laser scans were adjusted separately as well as k) 4 and l) 5 fisheye images as comparison. Calculations m) and n) combine the laser scans and fisheye images in an integrated adjustment.

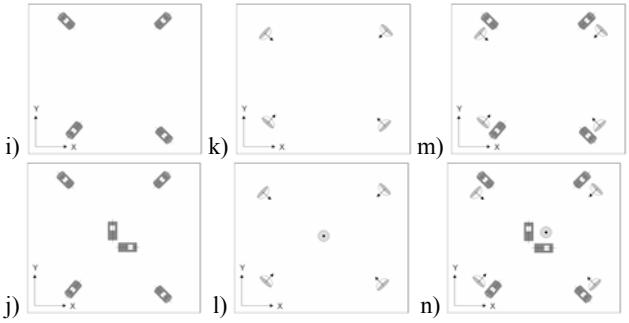

Figure 7. Configurations: multiple scans from the room corners

Applying configurations i) and j), which only use laser scanner observations, a slightly better accuracy (RMS of estimated standard deviations of object point coordinates) was achieved in comparison to calculation examples k) and l), which only use fisheye images for the 3D object point determination (table 3). But from table 3 it becomes obvious, that the combination of both leads to a significant improvement of the accuracy of object point coordinates. Calculations m) and n) show the potential of a combined processing of laser scanner and fisheye image observations.

	Scans/ Images	Observ./ Unknown	Points	RMS (mm) X	Y	Z	XYZ
i)	4 / 0	696 / 223	64	0.53	0.54	0.63	0.98
j)	6 / 0	1014 / 245	66	0.47	0.51	0.64	0.96
k)	0 / 4	472 / 232	66	0.75	0.72	0.59	1.20
l)	0 / 5	568 / 238	66	0.64	0.57	0.63	1.06
m)	4 / 4	1157 / 263	66	0.29	0.30	0.40	0.58
n)	6 / 5	1534 / 285	66	0.28	0.27	0.36	0.53

Table 3. Bundle adjustment results (configuration i – n)

4.5 Calibration results

An advantage of the processing of observations in a bundle adjustment is the possibility of self-calibration. This means that the used measurement device (laser scanner and/or camera) can be calibrated simultaneously, since the calibration parameters can be handled as unknowns in the same procedure. This was applied successfully in the calculation examples presented above.

Table 5 shows those laser scanner and camera calibration parameters, which could be determined significantly from the calculation examples j), l) and n). While j) and l) consider laser scanner and fisheye lens camera separately, calculation n) integrates both in one calculation. In addition to the parameter values their estimated standard deviation and significance level (in brackets) is presented.

Concerning the laser scanner only a few parameters could be determined significantly: The sine coefficient of vertical circle eccentricity (c_1) is most significant in calculation j). The horizontal and vertical collimation axis eccentricity (b_5, c_3) could be determined on a 99% significance level; their significance was increased in calculation n). While the trunnion axis error (b_2) and the vertical circle index error (c_0) could not be estimated significantly at all, the collimation axis error (b_1) was determined on a very low significance level. Additional parameters for the compensation of distance errors (offset a_0 and scale a_1) were included, too. Due to a high correlation between the two parameters, their significance is low. It might have been reasonable to omit one of both.

Also fisheye lens camera calibration parameters (interior orientation and additional parameters) were estimated, although not all of them are presented in table 5 (lens distortion parameters are rather uncritical herein in terms of correlations). The standard deviation of the principal distance c and the principal point coordinate y_0' could be improved in calculation n). The same applies to most of the additional parameters (distortion, affinity and shear).

It can be summarized, that the integrated processing of laser scanner data and fisheye image data (calculation n) results in calibration values, which have a higher accuracy and significance in comparison to calculation j) with scanner data and l) image data separately. That means that scanner and camera aid one another successfully in the self-calibration process.

	j)	n)
a_0 [10^{-3} mm]	4.00 ± 2.23 (90 %)	5.09 ± 2.18 (98 %)
a_1 [10^{-3}]	1.60 ± 0.64 (98 %)	1.37 ± 0.63 (95 %)
b_1 [10^{-3} rad]	2.91 ± 1.79 (80 %)	1.94 ± 1.54 (-)
b_5 [10^{-3} mm]	1.50 ± 0.51 (99.0 %)	1.58 ± 0.46 (99.9 %)
c_3 [10^{-3} mm]	2.86 ± 1.02 (99.0 %)	3.97 ± 0.88 (99.9 %)
c_1 [10^{-3} rad]	0.85 ± 0.09 (99.9 %)	0.97 ± 0.08 (99.9 %)
	l)	
c [mm]	8.011 ± 0.006	8.007 ± 0.002
x_0' [10^{-3} mm]	-153.9 ± 1.2 (99.9 %)	-153.7 ± 1.3 (99.9 %)
y_0' [10^{-3} mm]	-72.7 ± 3.7 (99.9 %)	-75.2 ± 1.8 (99.9 %)

Table 5. Estimated additional calibration parameters of laser scanner and fisheye lens camera

Own independent investigations have shown that the laser scanner calibration values vary due to different measurement conditions (distance range, scan resolution, target design, etc.). Therefore it is reasonable to implement the self-calibration strategy into the laser scanner processing in order to obtain values, which are particularly effective under the measurement conditions at hand. Thus, the accuracy of the laser scanner data can be improved in general.

4.6 Variance component estimation results

Table 6 shows the estimated a-priori standard deviations of the observation groups as a result from the bundle adjustment with variance component estimation (Schneider & Maas, 2007) of example j), l) and n). The observations are separated in distance D, horizontal and vertical scan angle α, β and image coordinates x', y'. These values provide information on the accuracy of the observations, which depends on the accuracy and stability of the used instrument, on the measurement conditions as well as on the correctness of the geometric model used for the calculation.

	j)	l)	n)
D	8.75 mm	-	8.68 mm
α	15.0 mgon	-	14.9 mgon
β	15.3 mgon	-	15.1 mgon
x', y'	-	0.228 pixel	0.176 pixel

Table 6. Estimated variance components of observations

It can be seen that the estimated standard deviations of each observation group were slightly improved in the integrated processing. The reason of this reduction is the higher reliability of the results due to different types of observations which are able to control each other within the bundle adjustment, i.e. outliers can be detected easier. Therefore a few more observations have been identified as outliers in calculation (n) in comparison to (j) and (l). This fact causes an improvement of the standard deviation of the observations as well as a slight improvement of the standard deviations of the unknown parameters.

5. CONCLUSIONS

Terrestrial laser scanner and fisheye lens camera complement one another quite well in an integrated processing scheme. Application-wise, a terrestrial laser scanner is mainly used for 3D modelling by an object representation based on stochastic distributed points, while a camera image is used for coordinate determination of discrete points as well as colorization of laser scanner point clouds or texturization of 3D models.

The simultaneous bundle adjustment of laser scanner and fisheye image observations as presented in this paper provides numerous advantages. One advantage of this approach is, that the camera can be orientated and calibrated on-site, which promises an optimal registration between both data sets. Furthermore, the camera can not only be used for providing colour information, but it is also able to participate in the determination of object geometries in terms of coordinates of object points in a multi-station configuration. Depending on the image resolution and camera stability, the camera even has the potential to improve the accuracy of 3D object points in comparison to the pure laser scanner measurement and to support the self-calibration of the laser scanner and thus to increase the accuracy of the laser scanner point cloud in general.

Due to different types of observations used in one calculation process, the reliability of the parameter and coordinate determination can be enhanced. The observations control each other, resulting in improved outlier identification.

Strictly spoken, the results and the drawn conclusions presented in this paper only apply to the actual recording and analysis parameters (scan resolution, sub-pixel image measurement of signalised points, etc.). Nevertheless, the potential of the presented approach (in terms of instrument calibration, sensor registration, enhancement of accuracy and reliability) has been shown.

In practical applications it is recommended to choose the laser scanner positions according to optimal visibility of the object details without occlusions and to capture a few fisheye images additionally, either from the same position as the laser scanner (if the camera is mounted on the laser scanner) or from different positions allowing for an optimal intersection geometry.

Finally it has to be noted that these conclusions also apply for conventional central perspective images, but with the limitation of a smaller field of view in comparison to fisheye images.

REFERENCES

Abraham, S., Förstner, W., 2005. Fish-eye-stereo calibration and epipolar rectification. ISPRS Journal of Photogrammetry & Remote Sensing, Vol. 59 (2005), 278-288.

Bakstein, H., Pajdla, T., 2002. Panoramic Mosaicing with a 180° Field of View Lens. In Proceedings of the IEEE Workshop on Omnidirectional Workshop, pp. 60-67, IEEE press.

Beers, B.J., 1997: 3-D landsurveying using the FRANK method: CycloMedia Mapper. In: Gruen/Kahmen: Optical 3-D Measurement Techniques IV. Wichmann Verlag, pp. 283-290.

Böhler, W., Marbs, A., 2004: Vergleichende Untersuchung zur Genauigkeit und Auflösung verschiedener Scanner. Luhmann, Müller (Hrsg.): Photogrammetrie, Laserscanning, Optische 3D-Messtechnik – Oldenburger 3D-Tage 2004, Wichmann Verlag.

Brown, D., 1971. Close-Range Camera Calibration. Photogrammetric Engineering, Vol. 37, No. 8.

El-Hakim, S.F., 1986. Real-Time Image Meteorology with CCD Cameras. Photogrammetric Engineering and Remote Sensing, Vol. 52, No. 11, pp. 1757-1766.

FARO Europe GmbH & Co. KG, 2005. Brochure FARO Laser Scanner LS. http://www.faro.com/coloroption/ (accessed 23 April 2008)

Jansa, J.; Studnicka, N.; Forkert, G.; Haring, A.; Kager, H., 2004: Terrestrial laserscanning and photogrammetry – acquisition techniques complementing one another. XX ISPRS Congress, Istanbul 2004, IAPRS Vol. XXXV, Part B5.

Lichti, D., 2007: Error modelling, calibration and analysis of an AM-CM terrestrial laser scanner system. ISPRS Journal of Photogrammetry & Remote Sensing 61 (2007) 307-324.

Luhmann, T., Hastedt, H., Tecklenburg, W., 2006: Modelling of chromatic aberration for high precision photogrammetry. Image Engineering and Vision Metrology, Proceedings ISPRS Com. V Symposium, IAPRS. Vol. XXXVI, Part 5.

Ray, S. F., 1994. Applied photographic optics – lenses and optical systems for photography, film, video and electronic imaging. 2nd Edition, Focal Press.

RIEGL Laser Measurement GmbH, 2007. Data Sheet LMS-Z420i. http://www.riegl.com/terrestrial_scanners/lms-z420i_/420i_all.htm (accessed 23 April 2008)

Rönnholm, P., Honkavaara, E., Litkey, P., Hyyppä, H., Hyyppä, J., 2007: Integration of laser scanning and photogrammetry. ISPRS Workshop on Laser Scanning and SilviLaser, Espoo, Finland, IAPRS Vol. XXXVI 3/W52.

Schneider, D.; Maas, H.-G. (2007): Integrated bundle adjustment with variance component estimation - fusion of terrestrial laser scanner data, panoramic and central perspective image data. ISPRS Workshop on Laser Scanning and SilviLaser 2007, Espoo (Finnland), IAPRS Vol. XXXVI, Part3/W52

Schwalbe, E., 2005. Geometric Modelling and calibration of fisheye lens camera systems. 2nd Panoramic Photogrammetry Workshop, Berlin. IAPRS Vol. XXXVI, 5/W8.

Schwalbe, E., Schneider, D., 2005. Design and testing of mathematical models for a full-spherical camera on the basis of a rotating linear array sensor and a fisheye lens. Grün, A; Kahmen H. (Eds.): Opt. 3-D Meas. Techn. VII. Vol. I: 245-254.

Ullrich, A., Schwarz, R., Kager, H., 2003: Using hybrid multi-station adjustment for an integrated camera laser-scanner system. Opt. 3-D Meas. Techniques VI, Vol. 1 (2003), 298-305.

van den Heuvel, F., Verwaal, R., Beers, B., 2006. Calibration of fisheye camera systems and the reduction of chromatic aberration. Proceedings ISPRS Commission V Symposium, IAPRS Vol. XXXVI, Part 5.

Wendt, A., Heipke, C., 2006: Simultaneous orientation of brightness, range and intensity images. IAPRS Vol. XXXVI, Part5.